Astronomy & Astrophysics manuscript no. Maglione
June 20, 2011

LETTER TO THE EDITOR

Simulation of dark lanes in post–flare supra–arcades

III. A 2D simulation

L. S. Maglione[1], E. M. Schneiter[2], A. Costa[2,3,4,⋆], and S. Elaskar[3,4]

[1] Facultad de Ingeniería, Universidad Nacional de Río Cuarto, Argentina
[2] Instituto de Astronomía Teórica y Experimental, Córdoba, Argentina
[3] Facultad de Ciencias Exactas, Físicas y Naturales, Universidad Nacional de Córdoba, Argentina
[4] Consejo Nacional de Investigaciones Científicas y Técnicas

Received ; accepted

ABSTRACT

Context. Using two simulations of $1.5D$, for the first time, in Costa et al. (2009) and Shulz et al. (2010) we numerically reproduce the observational dark inflows described in Verwichte et al. (2005). We show that the dark tracks can be explained as hot plasma vacuums generated upstream of a slow magnetoacoustic shock wave produced by a localized deposition of energy.
Aims. To confirm the later 'dark lane' interpretation and to identify specific $2D$ contributions to the description of the phenomenon.
Methods. To solve the ideal and non–stationary MHD equations we used a $2D$ Riemann solver Eulerian code specially designed to capture supersonic flow discontinuities.
Results. The numerical $2D$ results are in agreement with the observational behaviour however they show a slight shift in the characteristic parameter with respect to those found previously.
Conclusions. We confirm qualitatively the behaviour found in the previous papers. For a given numerical domain the period of the kink–like structure is a function of the magnetic field intensity: larger periods are associated with lower magnetic field intensities. Contrary to the $1D$ result -where the sunward dynamic is independent of the magnetic field intensity due to its exclusively waveguide role- in the $2D$ simulation the sunward speed is larger for larger values of the magnetic field. This can be interpreted as the capability of the low coronal plasma to collimate the deposition of energy into the magnetic field direction. The moving features consistent of low–density and high–temperature plasma cavities have larger inside values of the structuring parameter β than the neighboring media. Thus, the voids seem to be the emergence structures of a whole nonlinear interacting plasma context of shocks and waves more than voided plasma loops magnetically structured.

Key words. Corona, magnetic fields, shock waves, instabilities

1. Introduction

Dark sunward sinuous lanes moving along a fan of rays above post–flare loops towards a supra–arcade have been extensively studied (Innes et al. 2003a; 2003b; McKenzie and Savage 2009). The down moving structures observed at [40 – 60]Mm heights above the top of arcades, with a decelerating speed in the range $\sim$ [50 – 500]kms^{-1} were interpreted as sunward voided flows generated by reconnection processes developed by a current sheet above the flare arcade. Another configuration consistent with the observations is a magnetic flux tube, filled with flux and very little plasma, shrinking into the post-eruption arcade (McKenzie and Hudson 1999; McKenzie 2000). Recently Linton et al. (2009), proposed another description where the dynamic is triggered by a localized reconnection event that produces up and down flowing reconnected flux tubes which decelerate due to a underlying magnetic arcade loops. Verwichte et al. (2005, hereafter VNC) analyzed transverse to the magnetic field oscillations associated with sunward dark lanes in a post–flare supra–arcade. They found that the initial speeds and the displacement amplitudes, of observational dark lanes of a kink–like type, decrease as they propagate downwards while the period remains constant with height. increase.

⋆ CA: Andrea Costa, acosta@mail.oac.uncor.edu

In Costa et al. (2009) and in Schulz et al. (2010) (hereafter Paper 1 and 2, respectively), by the integration of two $1.5D$ MHD ideal equations, we presented a new scenario that gives account of the observational dark voids described in VNC. We simulated the effects of an initial impulsive and localized deposition of energy -supposed to be associated with above reconnection processes- in a plasma structured by sunward magnetic field lines. The impulsive phase was modeled by a pressure perturbation that initiates two main processes, a fundamentally hydrodynamic shock pattern directed sunwards and a perpendicular magnetic shock one, i.e., transverse to the magnetic field. The two patterns were supposed to be independent processes, however linked by their common origin and background magnetic and density conditions. The independence of the two dynamics was justified due to the far more effective conductive energy transport along field lines than across them.

We showed that the dark tracks are consistent with plasma voids generated by the bouncing and interfering of shocks and expansion waves upstream the initial localized deposition of energy, which is responsible of the two dynamics. The composition of both, a resulting sunward directed hydrodynamic shock pattern and a perpendicular magnetic shock one, produces an overall $\beta > 1$ transversely shaking void moving towards the sun surface, that resembles the kink–like mode described in VNC.

From the transverse simulation we found that, in accordance with the shock wave theory of uniform media (Kirk et al. 1994), there is a critical value of the magnetic field beyond which the behaviour of the magnetic shock pattern changes, the magnetic compression is limited and the phenomenon is progressively saturated. We also found that the period of the kink–like structure is a function of the magnetic field intensity while the amplitude is a function of the triggering pressure pulse. Thus, the period's constancy with height found in VNC can be associated with the almost constancy with height of the background magnetic field in the region. In accordance with our interpretation that in the sunward direction the magnetic field plays the role of being a wave–guide, we found that the pressure pulse determines an hydrodynamic shock that moves towards the sun surface at slow acoustic speed values and the dynamic is independent of the magnetic field intensity.

In this paper we investigate the goodness of the 1D model and we discuss the limitations and new characteristics of the phenomenon associated to the 2D structure.

2. Numerical Code and Initial Conditions

We integrate the MHD equations using the two-dimensional version of the 'Mezcal' code, an Eulerian Godunov MHD code (De Colle and Raga 2005, 2005, De Colle and al. 2008). The MHD Riemann solver uses a standard second-order Runge-Kutta method for the time integration and a spatially second-order reconstruction of the primitive variables at the interfaces (except in shocks). The constrained transport method (e.g., Tóth 2000) is used to conserve $\nabla \cdot \boldsymbol{B} = 0$ to machine accuracy. The code has been extensively tested against standard problems (De Colle 2005).

All calculations were performed using a numerical grid of $(x, y) = (1600, 620)$ grid–points corresponding to a physical size of $(40, 9)$Mm, chosen in accordance with VNC observations. The coordinate x represents the sunward direction and the y coordinate the transverse to the magnetic field one, as seen by the line of sight. We assumed a constant radial initial magnetic field structure, a typical background temperature of $T = 3.0 \times 10^6$K and a numerical density value of $\rho = 0.46 \times 10^9$ cm^{-3}. A spherical (circular in 2D) relative triggering pressure pulse P_2/P_1 (P_2 is the triggering pressure pulse and P_1 is the background gas pressure of the corona) of radius 0.6Mm was localized in the position $(1520, 434)$ equivalent to $(38, 6.3)$Mm.

Several simulation were carried out, varying the radial (normal to the sun's surface) magnetic field, B, and the localized deposition of energy, modelled as the relative triggering pressure pulse. As in Paper 1 and 2, the boundary conditions were fixed, allowing rebounds in the lateral transverse directions and also in the upper radial direction, resembling the action of the reconnection site. We assumed that the perturbations are absorbed in the sunward direction. The characteristic parameters were chosen in accordance with typical observed dark lane structures, e.g., VNC data and McKenzie and Hudson (1999).

3. Results and Discussion

Figures 1a,b show the density pattern in the central transverse direction and respectively, in the central longitudinal direction, as a function of time for $P_2/P_1 = 100$ and $B = 4$G. The figures are qualitatively similar to the $1D$ simulations (see Paper 1 and 2). The transverse kink–like structure is discontinued at a time step $\sim$ 80sec apparently due to a strong shock front that has swept material locally erasing the vacuum trace. These features -that remind observational constrictions, see e.g., Innes et al. (2003)a; (2003)b- were found in several cases at different positions and times, they are the result of nonlinear interactions difficult to predict. For further comparison we varied the background magnetic field. Table 1 shows the numerical periods (τ), amplitudes (A), the distances evacuated by the moving perturbations (L_v), and the initial sunward speeds (V_0) obtained for the 2G, 4G, 8G and 20G cases and for $P_2/P_1 = 100$. These results are consistent with characteristic observational values given in literature, e.g., VNC, McKenzie and Hudson (1999). However, in order to match periods of decades of seconds and amplitudes of hundreds of kilometers we required pressure pulses of almost an order of magnitude larger than in the $1D$ case. As before, we found that lower values of the magnetic field are associated with larger periods (see second column of Table 1). Also, the phenomenon is progressively saturated resembling the compressional limits (in density and magnetic field intensity) of the HD and transverse MHD shock wave theory in uniform medium (Kirk et al. 1994), i.e., the augmentation of the magnetic field from 4G to 6G implies a decrease of 55sec in the period while the change of magnetic field from 8G to 20G implies a decrease of only 10sec in the period. There is no visible relation between the magnetic field and the amplitude.

Figure 1c represents the void density for the longitudinal dynamic of the 20G magnetic field. Contrary to the sunward behaviour found in the $1D$ simulations, when comparing Fig. 1c with the 4G case of Fig. 1b, the void associated with larger magnetic field intensities travels a larger distance in the sunward direction (see Table 1, fourth column). In Paper 2, the hypothesis of independence between the two $1D$ simulations was justified by the anisotropy imposed by the magnetic field, thus its role was solely to wave guide the longitudinal dynamic. In the $2D$ simulation the deposition of energy is distributed radially, from the location of the initial perturbation, to all directions of the (x, y) plane. However, the freezing in of the plasma to the magnetic field induces the collimation of part of the energy towards the longitudinal direction. The more intense magnetic fields are the more efficient in line–tying the energy, thus, giving impulse to the final resulting sunward motion. Hence, the larger the magnetic field the more accurate the $1D$ description will be.

Figure 2a-d shows, respectively the 'dark lane' density structure, the temperature, the parameter β and the total pressure displayed in the whole numerical domain for 4G and $P_2/P_1 = 100$ at $t = 200$sec. As in Papers 2, in accordance with observational data, the vacuum density is almost an order of magnitude less than the external medium (see Fig. 3a), while the vacuum temperature is almost an order of magnitude higher than the temperature in the surroundings. When plotting β we see an extended channel (not confined to the vacuum zone) of inner β values lower than the outside ones. This behaviour occurs for the other cases, with different magnetic field intensities. Figure 3a shows the ratio of an average inner to an average outer β value for the different cases studied at a fix height of 35Mm. This indicates, as in Paper 2, that the inner magnetic pressure is not responsible of preventing the collapse of the vacuum zone. Furthermore, from Fig. 2d, it is possible to see that the features that characterize the vacuum zone have disappeared meaning that the contour of the cavity is, on average, in total pressure equilibrium. This confirms that the void dynamics must be sustained by the interaction of nonlinear waves and shocks acting in times comparable to the observations. For a more detailed description Fig. 3b shows respectively, the gas, the magnetic and the total pressure at each point corresponding to the line traced in Fig. 2a. Note that the

$B[G]$	$\tau[sec]$	$A[km]$	$L_v[Mm]$	$V_o[km/sec]$
4	80	725	22	200
6	25	825	24	250
8	20	825	26	259
20	10	750	40	280

Table 1. Numerical $2D$ parameters. ***B*** the magnetic field in the radial direction, τ the period, A the amplitude, L_v the distance evacuated by the perturbations and V_o the initial sunward speed. $P_2/P_1 = 100$G.

P_2/P_1	$\tau[sec]$	$A[km]$	$L_v[Mm]$	$V_o[km/sec]$
50	20	375	12	140
100	25	1000	24	259
150	25	750	23	280
200	−−	1875	32	318

Table 2. Numerical $2D$ parameters. P_2/P_1 the triggering pressure pulse, τ the period, A the amplitude, V_o the initial sunward speed and L_v the distance evacuated by the perturbations. For all cases $B = 8$G.

almost constancy of the total pressure is due to the gas pressure increase (which can only be accomplished through large temperature values) accompanied of a magnetic pressure decrease through the vacuum region.

In Paper 2 we found that the cases studied had $\beta > 1$, whereas in the $2D$ simulations only the cases with magnetic fields lower than 3G have $\beta > 1$. However, as in the $1D$ case, the behaviour is explained by the fact that β is larger inside than outside the voided cavity, i.e., the cavity is a result of dynamic nonlinear interacting waves and shocks sustaining the whole pattern. Note the differentiated shape of the Fig. 3a curve. The almost constant value of the curve for large values of the magnetic field intensity indicate a uniform behaviour within this range. The steep negative slope of large inner values of β and small values of the magnetic field, up to $B \sim 3$G, exhibit a dynamic where the anisotropy imposed by the magnetic field is softened and $2D$ features become more significant. However, magnetic field intensities lower than $B \sim 2.5$G have non–perturbed $\beta > 1$ values which are not realistic parameters for the low corona description. We conclude that the two $1D$ simulations give a good approximate description of the phenomenon.

Four runs, with different P_2/P_1, were carried out to analyze the behaviour of the voids. Table 2 shows the periods τ, the amplitudes A, the distances evacuated by the perturbations L_v, and the initial speed for a magnetic field intensity of 8G as a function of P_2/P_1. The obtained parameters are in correspondence with typical observed parameter ranges (see Table 1 in VNC). Note that from Table 2 we see that, as in Paper 2, the increase of P_2/P_1, implies the increase of the initial speed and the distance evacuated by the perturbation, whereas the periods and amplitudes show no regular variation.

4. Conclusions

We performed a $2D$ numerical simulation to reproduce observed dark sinuous lanes moving sunwardly towards supra–arcades. In previous papers we reproduce observational features of the phenomenon using two $1D$ simulations -supposed to be independent due to the far more effective transport along the field lines than across them- that were triggered by a pressure pulse acting on the transverse and longitudinal directions. The correspondent trans-

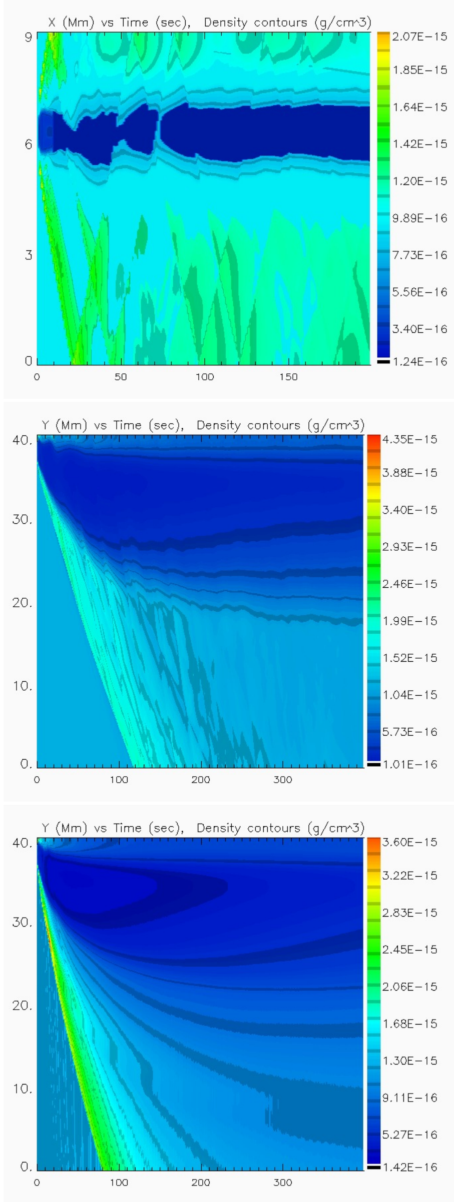

Fig. 1. Density patterns (gcm^{-3}) a) transverse kink–like oscillation of the dark lane as a function of time for 4G. b) and c) sunward motion as a function of time for 4G and 20G, respectively. $P_2/P_1 = 100$G.

verse and longitudinal patterns obtained from the $2D$ simulation are in good agreement with the observations, confirming that the two $1D$ description is suitable for this phenomenon.

The features, travelling decades of Mm, are voided cavities that elongate towards the sun decelerating at sounds speeds, i.e., at hundreds of kms^{-1}. The $2D$ results shown in Table 1 reproduce typical periods, amplitudes, distances travelled by the perturbations and their initial speeds. However, the pressure pulse required is almost an order of magnitude higher than in the $1D$ simulations. This seems reasonable due to the fact that the pulse must trigger the dynamic in all the radial directions and not only in two main ones. As shown in Table 2, the increase of the pressure pulse that triggers the phenomenon augments the initial speed and the distance travelled by the front of the voided cavity. Linton et al. (2009) also reproduce the sunward motion though they assume open lateral boundaries and a bottom reconnection

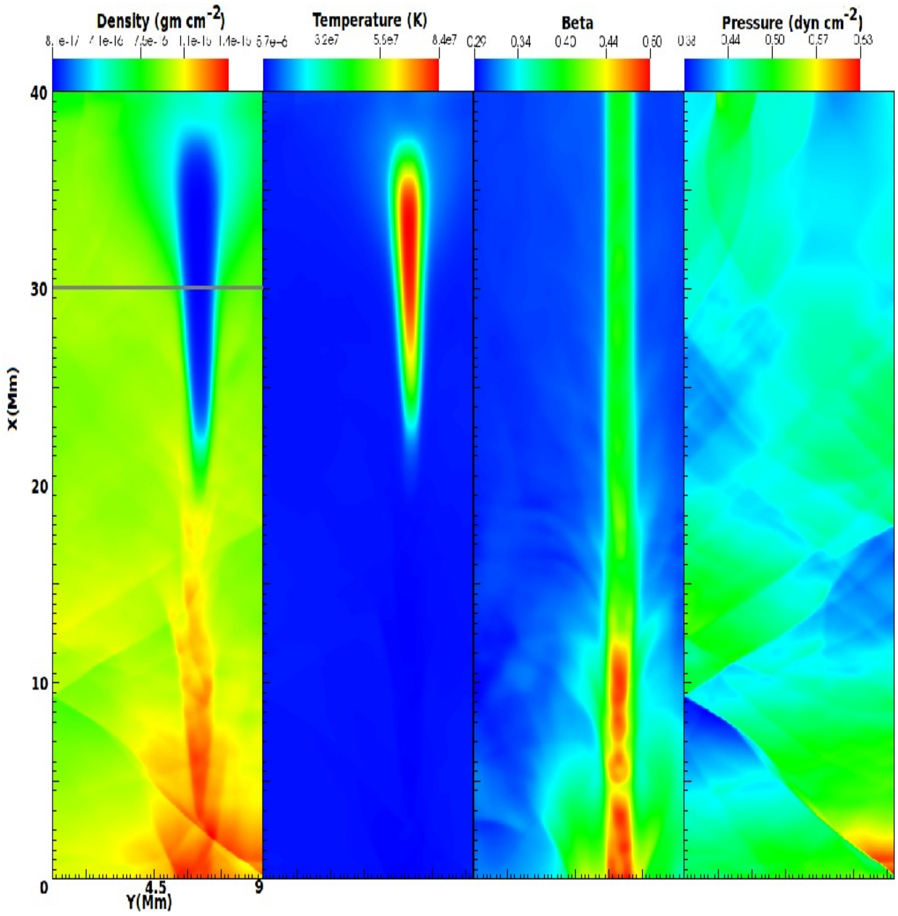

Fig. 2. a) density, b) temperature, c) β parameter and d) total pressure of the dark lane pattern. For all the cases we used the (x, y) grid defined as in VNC, x the radial direction and y the transverse direction, the magnetic field is 4G, the time is 200sec, and the triggering pulse is $P_2/P_1 = 100$G.

site. A main difference with our work is that the reconnection process is intrinsic to their model as the voids are formed and confined by a current sheet. From their work is not clear if an oscillating behaviour, as described in VNC, is obtained.

As in earlier works, we found that lower values of the magnetic field are associated with larger transverse periods. Also, we find from the behaviour of the period that, beyond a critical magnetic field value (between 4G and 6G), the phenomenon is progressively saturated with increasing values of the magnetic field. This reminds the compressional limits, in density and magnetic field intensity, of the HD and MHD shock wave theory for uniform media. However, the determination of the critical magnetic field value of this more complex scenario might be conditioned by other parameters not taken into account in this work such as the distance between the radial boundaries and the radius and the shape of the perturbation. The freezing in of the plasma to the magnetic field induces the collimation of part of the energy towards the sunward direction. Hence, larger magnetic field intensities produce features travelling farther.

Due to the fact that β is larger inside than outside the voided cavity, and that its contour is in total pressure equilibrium we conclude that the internal magnetic pressure cannot be responsible of preventing the collapse of the vacuum zone.

The $2D$ simulation shows, as in recent papers, that the sunwardly moving shaking voids are produced and sustained by two main processes that can be viewed as almost independent phenomenon if the magnetic field intensity is sufficiently high: 1) the interaction of nonlinear waves and shocks that rebound in the lateral denser medium, and 2) the interaction of nonlinear waves and shocks that upwardly rebound and are absorbed sunwardly.

References

Costa, A., Elaskar, S., Fernández, C., Martínez, G., MNRAS 400, L85, 2009
De Colle, F., Raga, A.C., MNRAS 359, 164, 2005
De Colle, F., Raga, A.C., A&A 449, 1061, 2006
De Colle, F., Raga, A.C., Esquivel, A., ApJ 689, 302, 2008
De Colle F., 2005, PhD thesis, UNAM
Fernández, C., Costa, A., Elaskar, S., Shulz, W., MNRAS, 400,1821,2009
Innes, D.E., McKenzie, D., Wang, T., Sol.Phys. 217, 247, 2003
Innes, D.E., McKenzie, D., Wang, T., Sol.Phys. 217, 267, 2003
Kirk, J., Melrose, D., Priest, E., ‘Plasma Astrophysics’ (Berlin, Verlag), 1994
Linton, M.G., DeVore, C.R., Longcope, D.W., Earth Planets Space, 61, 1, 2009
McKenzie, D., Sol.Phys. 195, 381, 2000
McKenzie, D., Hudson, H., ApJ, 519, L93, 1999
McKenzie, D., Savage, S., ApJ 697, 1569, 2009
Schulz, W., Costa, A., Elaskar, S., Cid, G., MNRAS, 407, L89, 2010
Tóth G., 2000, Journal of Computational Physics, 161, 605
Verwichte, E., Nakariakov, V., Cooper, F., A&A 430, L65, 2005

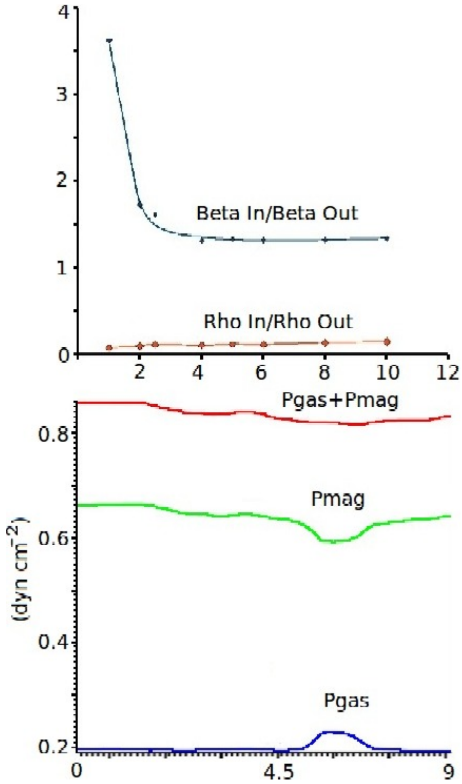

Fig. 3. a) β average inner to outer ratio values for different magnetic field intensity cases. b) gas, magnetic and total pressure values for the grid positions of the line marked in Fig. 2a and $B = 4$G. For all cases the triggering pulse is $P_2/P_1 = 100$G and $\tau = 200$.